Int. J. Sci. R. Tech., 2026 3(9)
A Multidisciplinary peer-reviewed Journal
www.ijsrtjournal.com [ISSN: 2394-7063]

Original Article

Waste-To-Wealth Valorization Of The Invasive Grass *Leersia Hexandra* Into Fluorescent Carbon Dots Via Microwave-Assisted Synthesis: Multi-Technique Characterization And DPPH Radical-Scavenging Potential

Shyamala Chandra Rokkala[1]*, Amal Joseph PJ[2]

[1]*Department of Biotechnology, SRR Government Arts & Science College (A), Karimnagar, Telangana, India.*
[2]*Department of Chemistry, Mahatma Gandhi Govt.Arts College, Mahe, Puducherry.*

ABSTRACT

Carbon dots (CDs) are zero-dimensional, quasi-spherical carbon nanostructures that have attracted enormous research interest owing to their tunable photoluminescence, low toxicity, aqueous dispersibility, and facile, low-cost synthesis from renewable precursors. In the present study, fluorescent carbon dots were synthesized in a single step from *Leersia hexandra*, an invasive perennial grass weed of paddy ecosystems, using a rapid, solvent-free microwave-assisted route (total irradiation time of 8 min, 640 W, pulsed 30 s on/30 s off), thereby converting an agronomic waste biomass into a value-added nanomaterial. The resulting carbon dots (LH-CDs) were purified by sequential filtration through muslin cloth, Whatman No. 1 filter paper, centrifugation and 0.22 µm nylon syringe filtration, and were characterized by UV-Visible absorption spectroscopy, Fourier-transform infrared (FTIR) spectroscopy, fluorescence spectroscopy and dynamic light scattering-based zeta potential analysis. UV-Vis analysis revealed characteristic $\pi \rightarrow \pi^*$ and $n \rightarrow \pi^*$ absorption features, from which direct and indirect optical band gaps of 3.75 eV and 2.13 eV were extracted using Tauc plots. FTIR confirmed a hydrophilic, oxygen/nitrogen-rich surface bearing hydroxyl, carboxyl and amine functionalities, while deconvoluted photoluminescence spectra revealed three overlapping emissive states centred at 527, 558 and 614 nm. Zeta potential measurement indicated a weakly negative surface charge of -3.26 ± 6.68 mV. The LH-CDs exhibited concentration-dependent DPPH free-radical scavenging activity comparable to, and at low concentrations exceeding, that of ascorbic acid, with an estimated half-maximal scavenging concentration below 1 µg/mL. These results revealed *L. hexandra* as an unexplored, abundant, and cost-free precursor for the green synthesis of antioxidant carbon dots, underscoring a practical waste-to-wealth strategy for agricultural weed management and functional nanomaterial development.

Keywords: Carbon dots; *Leersia hexandra*; microwave-assisted synthesis; waste-to-wealth; photoluminescence; DPPH antioxidant activity.

INTRODUCTION

Carbon dots (CDs) represent one of the most rapidly expanding classes of fluorescent carbon-based nanomaterials to have emerged in the last two decades. First isolated in 2004 during the electrophoretic purification of single-walled carbon nanotubes [1], CDs are typically defined as quasi-spherical carbon nanoparticles below 10 nm in size, comprising a graphitic or amorphous sp2/sp3 carbon core decorated with oxygen-, nitrogen- or sulfur-containing surface functionalities. Unlike traditional semiconductor quantum dots, which frequently contain toxic heavy metals such as cadmium or lead, carbon dots offer an intrinsically biocompatible, chemically inert and environmentally benign alternative while retaining many of the desirable optical attributes of quantum-confined nanomaterials, including size- and excitation-dependent photoluminescence, high photostability, large Stokes shifts and resistance to photobleaching. These properties have propelled carbon dots into an exceptionally broad application space encompassing bioimaging, drug delivery, optical sensing of metal ions and biomolecules, photocatalysis, anti-counterfeiting, light-emitting devices and,

Relevant conflicts of interest/financial disclosures: The authors declare that the research was conducted in the absence of any commercial or financial relationships that could be construed as a potential conflict of interest.

increasingly, biomedical antioxidant and antimicrobial therapeutics [2].

Among the various synthetic strategies developed for carbon dots, a fundamental distinction is drawn between "top-down" approaches, which fragment bulk carbon allotropes (such as graphite, carbon nanotubes or activated carbon) into nanoscale units via arc discharge, laser ablation or chemical/electrochemical oxidation, and "bottom-up" approaches, which assemble carbon dots directly from small organic molecules or biomass through carbonization, hydrothermal treatment, pyrolysis or microwave irradiation [5]. While early bottom-up syntheses relied heavily on petrochemical precursors such as citric acid, ethylenediamine or glucose, the last decade has witnessed a decisive shift toward green, biomass-derived precursor, driven by the twin imperatives of sustainability and cost reduction. Agricultural residues, fruit and vegetable peels, food wastes, herbs and even municipal or animal-derived biomass have all been successfully converted into fluorescent carbon dots [4], giving rise to the now widely used "waste-to-wealth" paradigm in carbon dot research [3]. This reframes waste biomass, which would otherwise require disposal or remain an ecological burden, as an inexpensive and renewable carbon source for high-value nanomaterials, thereby simultaneously addressing waste management challenges and expanding the sustainable materials portfolio available to nanotechnology.

Microwave-assisted synthesis has emerged as a particularly attractive bottom-up route within this green-chemistry framework [6]. Compared with conventional hydrothermal or solvothermal treatments, which typically require several hours at elevated temperature and pressure inside sealed autoclaves, microwave irradiation delivers rapid, volumetric and relatively uniform dielectric heating directly to the reaction mixture. This translates into markedly shorter reaction times (often minutes rather than hours), lower energy consumption, improved batch-to-batch reproducibility and a scalable, equipment-light protocol suitable for point-of-use synthesis. These advantages have made microwave-assisted carbonization one of the most frequently reported methods for converting plant-derived biomass into carbon dots in the recent literature, as exemplified by the rapid, single-step microwave synthesis of nitrogen-doped carbon dots from biomass precursors for sensing applications [7].

The choice of biomass precursor exerts a decisive influence on the surface chemistry, heteroatom doping level and, consequently, the functional performance of the resulting carbon dots. In this context, *Leersia hexandra* Sw. (commonly known as southern cutgrass, swamp rice grass or clubhead cutgrass) presents a compelling and, to date, unexploited precursor. *L. hexandra* is a perennial, rhizomatous aquatic grass that occurs pantropically across South and Southeast Asia, Africa and the Americas, and is agronomically classified as a persistent and troublesome weed of flooded and irrigated rice paddies, where it competes aggressively with the rice crop for nutrients, light and space and additionally serves as an alternate host for several rice pests and pathogens [8]. Because of its rhizomatous growth habit and vegetative propagation, *L. hexandra* forms dense, difficult-to-eradicate stands that are routinely removed as a matter of weed management and typically discarded without any value-added utilization. Its lignocellulosic composition, being rich in cellulose, hemicellulose and lignin as well as endogenous nitrogenous compounds, provides an abundant, renewable and essentially cost-free source of the carbon, oxygen and nitrogen atoms required for carbon dot nucleation and surface functionalization. Valorizing this troublesome weed into a photoluminescent, antioxidant nanomaterial therefore constitutes an especially apt illustration of the waste-to-wealth concept: a plant that is otherwise a net economic and ecological liability to rice cultivation is repurposed into a functional nanomaterial with demonstrable free-radical scavenging capability, thereby generating significant value from an agricultural waste while simultaneously incentivizing its removal from paddy ecosystems.

Beyond their well-documented optical and sensing applications, carbon dots have more recently attracted attention as non-enzymatic antioxidant agents capable of scavenging reactive oxygen species and stable free radicals such as 2,2-diphenyl-1-picrylhydrazyl (DPPH•). The antioxidant activity of carbon dots is generally attributed to the abundance of electron- and hydrogen-donating surface moieties, particularly hydroxyl, carboxyl and amine groups, acting in concert with the electron-rich, delocalized sp2

aromatic core, which together enable both hydrogen-atom-transfer (HAT) and single-electron-transfer (SET) mechanisms of radical neutralization [9], [10], [11]. Because green, biomass-derived carbon dots are frequently rich in exactly these functional groups, they are particularly well suited to antioxidant applications, offering a biocompatible, photostable and reusable alternative or adjunct to conventional small-molecule antioxidants such as ascorbic acid, which are prone to oxidative degradation and possess only a single mode of radical scavenging.

After thorough literature survey, the present study reports, for the first time, the synthesis of fluorescent carbon dots from *Leersia hexandra* grass biomass via a rapid microwave-assisted route.

2. MATERIALS AND METHODS

2.1. Materials

Fresh *Leersia hexandra* grass, distilled water, 2,2-diphenyl-1-picrylhydrazyl (DPPH) reagent, ascorbic acid (analytical grade), methanol (analytical/spectroscopic grade), muslin cloth, Whatman No. 1 qualitative filter paper, and 0.22 µm pore-size nylon syringe filters were used. All aqueous solutions were prepared using double-distilled water unless otherwise specified.

2.2. Plant Collection and Processing

Healthy specimens of *Leersia hexandra* were collected from local paddy habitats. The collected biomass was thoroughly washed under running water to remove adhering soil and debris, rinsed with distilled water, and shade-dried at room temperature. The dried biomass was subsequently pulverized using a laboratory grinder and passed through a fine mesh to obtain a homogeneous powder, which was stored in an airtight container until further use.

2.3. Microwave-Assisted Synthesis of Carbon Dots

Carbon dots were synthesized following a one-pot, solvent-free microwave-assisted carbonization protocol. Briefly, 5 g of the pulverized *L. hexandra* powder was dispersed in 100 mL of distilled water under continuous magnetic stirring at 120 °C until a homogeneous suspension was obtained. The dispersion was then subjected to microwave irradiation at 640 W for a cumulative duration of 8 min, delivered as intermittent pulses of 30 s irradiation followed by 30 s rest intervals, in order to promote controlled carbonization while minimizing thermal runaway and over-carbonization. Upon cooling to room temperature, the resulting dark brown colloidal suspension was sequentially purified: coarse plant debris was first removed by filtration through muslin cloth, followed by filtration through Whatman No. 1 filter paper to eliminate finer particulates. The filtrate was then centrifuged at 5000 rpm to sediment residual larger aggregates, and the supernatant was finally passed through a 0.22 µm nylon syringe filter to yield an optically clear, homogeneous colloidal solution of *L. hexandra*-derived carbon dots (LH-CDs), which was stored at 4 °C in the dark prior to characterization.

2.4. Characterization

The optical absorption properties of the LH-CDs were recorded on a UV-Visible spectrophotometer over the wavelength range of 200-800 nm. Surface functional groups were identified by Fourier-transform infrared (FTIR) spectroscopy over the 4000-400 cm^{-1} range. The photoluminescence (PL) behaviour of the LH-CDs was investigated using a fluorescence spectrophotometer, with the emission spectrum recorded following excitation in the near-UV region. The surface charge and colloidal stability of the LH-CDs were assessed by zeta potential measurement using a Malvern Zetasizer.

2.5. DPPH Free-Radical Scavenging Assay

The antioxidant capacity of the LH-CDs was evaluated using the DPPH free-radical scavenging assay, with ascorbic acid employed as the reference standard antioxidant. A methanolic stock solution of DPPH (3mM) was prepared and protected from light. Test solutions of both ascorbic acid and LH-CDs were prepared across a two-fold serial dilution series comprising nine levels: an untreated control (DPPH solution with no added antioxidant) and test concentrations of 1, 2, 4, 8, 16, 32, 64 and 128 µg/mL. For each concentration, an aliquot of the test solution (ascorbic acid or LH-CDs) was mixed with the DPPH methanolic solution in a fixed volumetric ratio and the mixture was incubated in the dark at room temperature for 30 min to allow the reaction to reach completion. Following incubation, the absorbance of each mixture was recorded in the 400-600 nm range

using a UV-Visible spectrophotometer, with particular attention to the characteristic DPPH absorption maximum located at approximately 515-520 nm, which corresponds to the deep-violet, radical (unreduced) form of DPPH. A progressive decrease in absorbance at this wavelength, accompanied by visual bleaching of the solution from violet toward pale yellow, indicates radical scavenging (reduction of DPPH• to the stable, diamagnetic DPPH-H species). The percentage DPPH scavenging activity at each concentration was calculated using the standard equation:

Scavenging activity (%) = [(A*control* − A*sample*) / A*control*] × 100

where A control is the absorbance of the DPPH solution in the absence of any test compound and A sample is the absorbance of the DPPH solution in the presence of ascorbic acid or LH-CDs at a given concentration. All spectral measurements were performed in triplicate, and mean values were used for subsequent analysis and plotting.

3. RESULTS AND DISCUSSION

3.1. UV-Visible Absorption Spectroscopy and Optical Band Gap

The UV-Visible absorption spectrum of the LH-CDs (Figure 1a) displayed a strong, monotonically decreasing absorption profile extending from the deep-UV region into the visible range, with a discernible shoulder centred near 240-245 nm and a weaker, broader shoulder around 285-295 nm. The higher-energy shoulder is consistent with the π→π* electronic transition of conjugated C=C bonds within the aromatic sp^2 carbon core, whereas the weaker, red-shifted shoulder is attributed to the n→π* transition of carbonyl (C=O) and related oxygen-containing surface functionalities, in agreement with previously reported biomass-derived carbon dot systems in which analogous π→π* absorption features have been located in the 220-270 nm region [12]. The absence of a sharp, well-resolved excitonic peak, together with the gradual absorption tail extending toward the visible region, is characteristic of the size and surface-state heterogeneity typical of polydisperse, biomass-derived carbon dots synthesized by rapid, uncontrolled thermal routes such as microwave carbonization.

To quantify the optical band gap of the LH-CDs, the absorption data were transformed according to the Tauc relation and plotted as $(Ahν)^2$ versus photon energy (hν) for the direct allowed transition (Figure 1b) and as $(Ahν)^{(1/2)}$ versus hν for the indirect allowed transition (Figure 1c). Linear extrapolation of the steep absorption-edge region to the photon-energy axis yielded a direct optical band gap of 3.75 eV and an indirect optical band gap of 2.13 eV for the LH-CDs. These values fall within the range typically reported for biomass-derived carbon dots. For instance, *Aouadi et al.* [13] reported direct and indirect band gaps of 3.65 eV and 3.47 eV, respectively, for carbon quantum dots synthesized from lemon peel extract, while a related study on *Opuntia ficus-indica*- and Agave-derived carbon quantum dots [12] reported a π→π* absorption band located near 220 nm associated with a comparably wide optical gap. The somewhat lower indirect band gap obtained for the LH-CDs relative to the citrus-derived systems may be rationalized by a larger average sp^2 conjugation domain size and/or a higher degree of surface passivation by oxygen/nitrogen heteroatoms, both of which are known to narrow the effective optical gap of carbon dots by introducing intra-gap surface trap states.

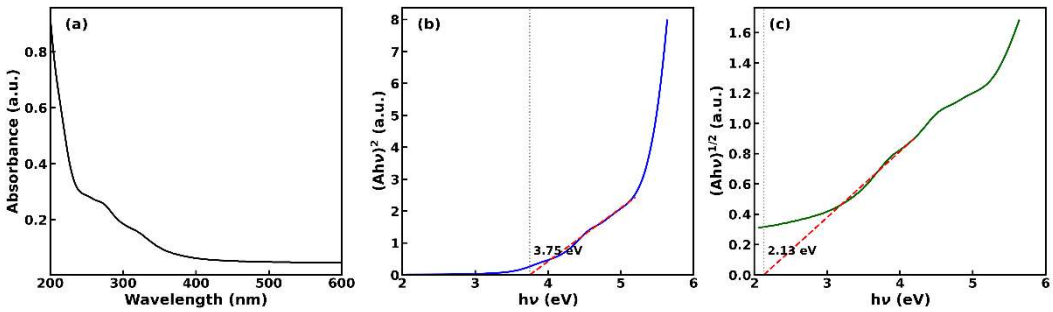

Figure 1. Absorption properties of *L. hexandra* carbon dots: (a) UV-Visible absorption spectrum, (b) direct band gap Tauc plot [(Ahν)² vs hν], and (c) indirect band gap Tauc plot [(Ahν)^1/2 vs hν].

3.2. FTIR Spectroscopy

The FTIR transmittance spectrum of the LH-CDs (Figure 2) revealed a rich set of vibrational bands consistent with a hydrophilic, oxygen- and nitrogen-functionalized carbon dot surface. A broad, intense band centred at 3309 cm^{-1} was assigned to overlapping O-H and N-H stretching vibrations, indicating an abundance of hydroxyl and amine/amide groups originating from the lignocellulosic and proteinaceous constituents of the grass precursor. A moderate band at 2982 cm^{-1}corresponded to aliphatic C-H stretching vibrations, while the prominent band at 1637 $cm^{-1}$was attributed to C=C skeletal stretching of the aromatic carbon core, overlapping with C=O stretching of amide/carbonyl moieties. The band at 1407 cm^{-1} was assigned to the symmetric stretching vibration of carboxylate ($-COO^{-}$) groups and/or C-N stretching, whereas the band at 1254 cm^{-1} was attributed to C-O-C/C-N stretching vibrations. A sharp, intense band in the 1000-1050 cm^{-1} region (labelled at 1030 cm^{-1}) was assigned to C-O stretching vibrations of residual polysaccharide-derived alcohol and ether linkages, and the weaker band at 587 cm^{-1} was attributed to out-of-plane bending vibrations of the aromatic ring skeleton. These assignments confirm that the surface of the LH-CDs is densely decorated with hydroxyl, carboxyl, carbonyl and amine functional groups, imparting excellent aqueous dispersibility and providing abundant sites for hydrogen-atom donation.

These findings similar to those reported for other microwave- and hydrothermally synthesized biomass-derived carbon dots. Springer/Carbon Research [7] reported analogous O-H/N-H stretching bands at 3130 and 3028 cm^{-1}alongside C=N and C-N bands near 1600 and 1100 $cm^{-1}$for microwave-synthesized, nitrogen-doped biomass carbon dots, while fennel-seed-derived carbon quantum dots [14] likewise exhibited dominant C=C, C=O and C-H vibrational signatures, with the disappearance of precursor-specific CH_2 bands confirming effective carbonization.

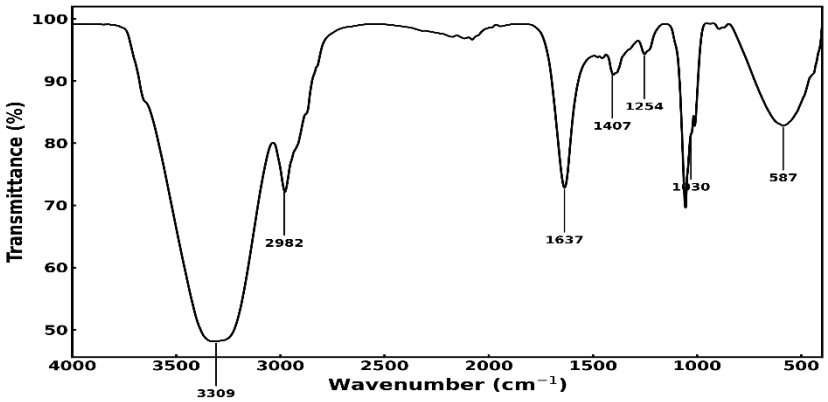

Figure 2. FTIR transmittance spectrum of *L. hexandra* carbon dots showing major vibrational assignments.

3.3. Fluorescence (Photoluminescence) Spectroscopy

The photoluminescence emission spectrum of the LH-CDs (Figure 3) exhibited a broad, asymmetric emission band spanning approximately 480-700 nm with an apparent maximum near 528 nm, indicative of green emission. Multi-Gaussian resolution of the emission envelope resolved three overlapping emissive components centred at 527, 558 and 614 nm. The dominant component at 527 nm is attributed to intrinsic, carbon-core-related radiative recombination coupled with the surface states of carbonyl/carboxyl groups, consistent with the well-documented association between -CO-OH-type surface groups and green emission (500-520 nm) in carbon dots. The intermediate component at 558 nm is ascribed to a distinct surface-trap emissive state, likely mediated by C-N and C-O surface moieties identified in the FTIR spectrum, while the weak, red-shifted component at 614 nm is attributed to lower-energy trap states associated with larger, more extended conjugated domains or partial nanoparticle aggregation. The coexistence of multiple, spectrally overlapping emissive states is a well-established phenomenon in biomass-derived carbon dots and generally reflects

the inherent structural and surface heterogeneity that accompanies rapid, one-pot carbonization of complex, multi-component biomass precursors.

This multi-emissive behaviour is consistent with previous reports. A study on N-, O-functionalized carbon dots [11] resolved a bright blue emission at 430 nm associated with N-rich pyridone/carbonyl moieties and a distinct, less intense green emission near 500 nm arising from C-N and C-O transitions and inter-system-crossing trap states, closely mirroring the multi-component emission architecture observed here. Similarly, fenugreek-seed-derived carbon quantum dots [15] were reported to exhibit two or more coexisting fluorescence mechanisms, with heteroatom doping and surface-active groups identified as the principal factors governing the resulting emissive states.

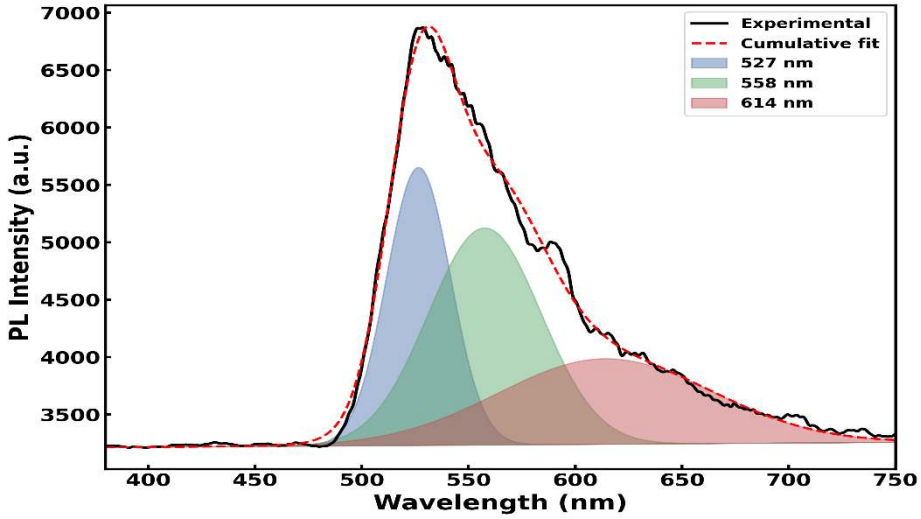

Figure 3. Photoluminescence emission spectrum of *L. hexandra* carbon dots and Gaussian emissive components centred at 527, 558 and 614 nm.

3.4. Zeta Potential Analysis

The zeta potential distribution of the LH-CDs (Figure 4) exhibited a single, well-defined Gaussian population with a mean zeta potential of −3.26 mV and a standard deviation of 6.68 mV, measured at a conductivity of 0.112 mS/cm. This weakly negative surface charge is consistent with partial ionization of surface carboxyl and hydroxyl groups (identified by FTIR at 1407 and 3309 cm^{-1}, respectively) under the aqueous measurement conditions. However, the magnitude of the zeta potential falls considerably below the ±30 mV threshold conventionally regarded as necessary for long-term electrostatic colloidal stability, suggesting that the aqueous LH-CD dispersion, while adequately dispersible for immediate spectroscopic and bioassay purposes, may be prone to gradual aggregation upon prolonged storage unless further surface modification or steric stabilization is introduced.

This value is markedly lower in magnitude than the zeta potentials reported for several other biomass-derived carbon dot systems. For example, a recent review of biomass-derived carbon dots for bioimaging applications [16] reported zeta potential values more negative than −30 mV for -OH/-COOH-rich carbon dots, indicative of high colloidal stability, while a structural investigation of multiple carbon dot types [17] reported zeta potentials of approximately −38 mV and −12.2 mV for two distinct biomass-derived carbon dot preparations, attributing the difference in aqueous stability directly to the magnitude of the surface charge despite similar surface functional group profiles.

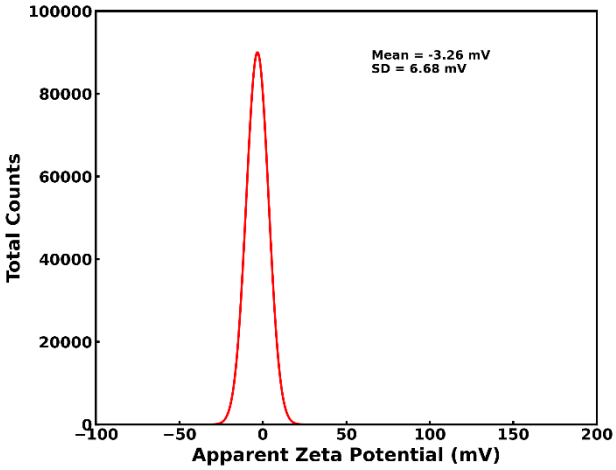

Figure 4. Zeta potential distribution of *L. hexandra* carbon dots.

3.5. DPPH Radical Scavenging Antioxidant Activity

Carbon dots have increasingly been recognized as effective non-enzymatic antioxidants capable of neutralizing stable free radicals such as DPPH•, owing to the combined action of an electron-rich, delocalized sp2 aromatic core and an abundance of hydrogen- and electron-donating surface functional groups. Because green, biomass-derived carbon dots are typically enriched in hydroxyl, carboxyl and amine moieties relative to carbon dots synthesized from purely synthetic precursors, they are particularly well positioned to serve as sustainable antioxidant nanomaterials, offering advantages of photostability and reusability over conventional small-molecule antioxidants.

The DPPH radical exhibits a characteristic deep-violet colour with strong absorbance centred near 515-520 nm, arising from the delocalized, resonance-stabilized free radical. Upon reduction to its diamagnetic form (DPPH-H), this absorbance diminishes and the solution visibly bleaches toward pale yellow. Figure 5 presents the UV-Visible absorbance spectra of the DPPH solution in the presence of increasing concentrations of ascorbic acid (1-128 µg/mL), while Figure 6 presents the corresponding spectra for the LH-CDs. In both cases, a clear, concentration-dependent suppression of the 515-520 nm absorption band was observed relative to the untreated DPPH control, confirming progressive radical scavenging by both the reference antioxidant and the synthesized carbon dots.

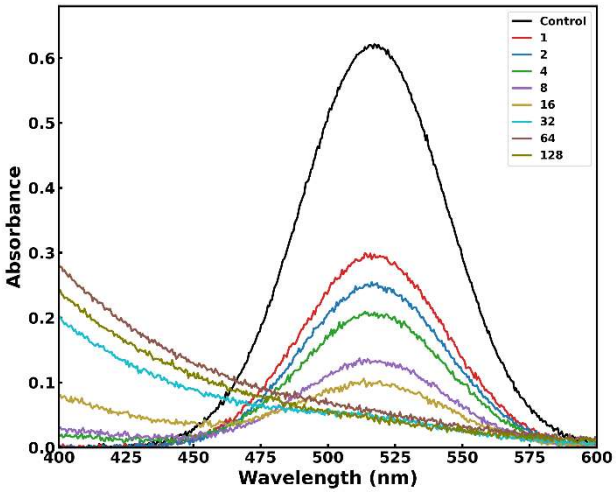

Figure 5. UV-Visible absorbance spectra of the DPPH assay in the presence of ascorbic acid at concentrations of 1-128 µg/mL.

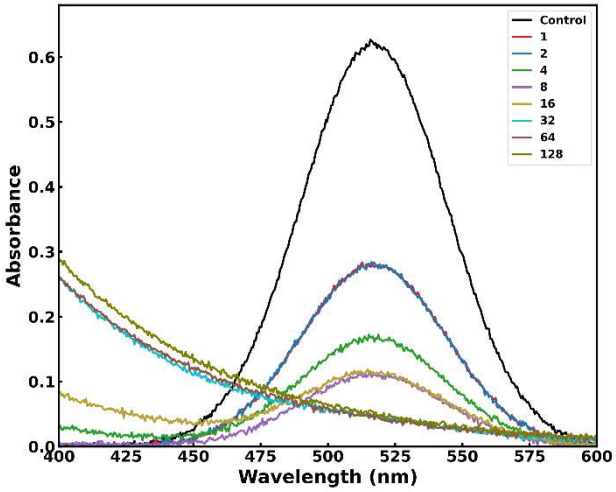

Figure 6. UV-Visible absorbance spectra of the DPPH assay in the presence of *L. hexandra* carbon dots at concentrations of 1-128 µg/mL.

The percentage DPPH scavenging activity calculated from the absorbance values at the DPPH absorption maximum is plotted as a function of concentration for both ascorbic acid and the LH-CDs in Figure 7. Both samples displayed the expected sigmoidal, concentration-dependent increase in scavenging activity, rising from approximately 48-51% at the lowest tested concentration (1 µg/mL) to greater than 95% scavenging at 64-128 µg/mL. Significantly, at low-to-intermediate concentrations (2-8 µg/mL), the LH-CDs exhibited scavenging activity equal to or modestly exceeding that of ascorbic acid, while at the highest concentrations both samples converged toward near-complete (>96%) radical neutralization. Interpolation of the dose-response curves yielded an estimated IC_{50} (half-maximal scavenging concentration) of approximately 1.2 µg/mL for ascorbic acid and below 1 µg/mL for the LH-CDs, indicating that the *L. hexandra*-derived carbon dots possess an antioxidant potency at least comparable to, and in the low-concentration regime slightly exceeding, that of the gold-standard reference antioxidant.

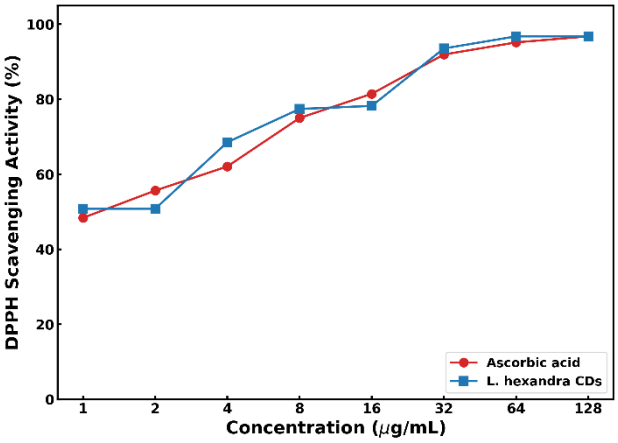

Figure 7. Concentration-dependent DPPH radical scavenging activity (%) of ascorbic acid and *L. hexandra* carbon dots.

This level of antioxidant potency is exceptional when benchmarked against previously reported biomass-derived carbon dot systems, most of which report IC_{50} values in the sub-milligram to milligram/mLe range rather than the low-microgram-per-millilitre range observed here. Pineapple-peel-derived carbon dots synthesized by a comparable microwave method were reported to exhibit a DPPH IC_{50} of 0.79 mg/mL [18], approximately three orders of magnitude higher (i.e., far less potent) than the LH-CDs. Citrus-peel-derived carbon quantum dots from lemon and orange were reported to possess DPPH IC_{50} values of 2.378 and

3.059 mg/mL, respectively [13], again substantially less potent than the present system. A comparative assessment of carbon-based nanomaterials from different sources reported an IC_{50} of 254.2 µg/mL for the most active iron-doped carbon dot formulation [19], still approximately 250-fold higher than that estimated for the LH-CDs, while *Houttuynia cordata*-derived carbon quantum dots exhibited an IC_{50} of approximately 0.9 mg/mL [20]. The closest literature comparator was found in carbon dot nanoparticles derived from *Medinilla speciosa* (Asian grape) peel, which displayed a DPPH IC_{50} of 6.89 µg/mL and 73.82% scavenging activity at 5 mg/mL [21]; although this value remains roughly seven-fold higher than the IC_{50} estimated for the LH-CDs.

3.6. Hypothetical Mechanism of DPPH Scavenging by LH-CDs

On the basis of the surface functional group profile established by FTIR and in accordance with mechanisms proposed for structurally related carbon dot systems, the antioxidant action of the LH-CDs against the DPPH radical is proposed to proceed predominantly via a hydrogen-atom-transfer (HAT) pathway, supplemented by a secondary single-electron-transfer (SET) contribution. The abundant hydroxyl and amine groups identified by the broad 3309 cm^{-1} O-H/N-H stretching band are proposed to act as the principal hydrogen donors, transferring a labile hydrogen atom to the nitrogen-centred DPPH• radical to generate the stable, diamagnetic DPPH-H adduct while the carbon dot surface oxygen/nitrogen atom is left as a comparatively stable, resonance-delocalized radical intermediate. This is consistent with several previous mechanistic studies, which have demonstrated that both carboxyl (-COOH) and amino ($-NH_2$) surface groups on carbon nanodots contribute to DPPH scavenging through direct or indirect hydrogen-atom-transfer reactions [22], [9], and that protonation of these groups under acidic conditions further enhances radical-scavenging efficiency by increasing the availability of transferable hydrogen atoms [9]. The carboxylate/carbonyl groups evidenced by the 1637 and 1407 cm^{-1} FTIR bands are proposed to act as auxiliary proton-donor sites, analogous to the mechanism described for N,S-co-doped carbon dots, in which surface groups transfer hydrogen atoms to counteract free radicals while the sp^2-conjugated aromatic core simultaneously facilitates electron mobility, enabling a complementary single-electron-transfer route to radical neutralization [10]. Furthermore, carboxyl groups on the LH-CD surface may additionally stabilize the DPPH-H adduct through the formation of a transient hydrogen-bonded or charge-transfer complex, a mechanism reported to be the primary source of antioxidation for structurally analogous carboxyl-rich carbon nanodots [23]. The concerted operation of these HAT and SET pathways across a densely functionalized, multi-group surface offers a plausible explanation for the unusually low IC_{50} observed for the LH-CDs relative to previously reported, less densely functionalized biomass-derived carbon dot systems.

CONCLUSION

Fluorescent carbon dots were successfully synthesized in a single, rapid step from *Leersia hexandra*, an invasive and economically burdensome paddy weed, via a solvent-free microwave-assisted carbonization route, demonstrating a practical and readily scalable waste-to-wealth valorization strategy. Comprehensive characterization confirmed the formation of small, oxygen/nitrogen-functionalized carbon dots exhibiting direct and indirect optical band gaps of 3.75 eV and 2.13 eV, a hydrophilic surface densely decorated with hydroxyl, carboxyl, carbonyl and amine groups, multi-state green photoluminescence resolved into three emissive components (527, 558 and 614 nm), and a weakly negative surface charge of −3.26 mV. Functionally, the LH-CDs exhibited pronounced, concentration-dependent DPPH free-radical scavenging activity, with an estimated IC_{50} below 1 µg/mL, a potency comparable to or exceeding that of the reference antioxidant ascorbic acid and substantially superior to the majority of previously reported biomass-derived carbon dot systems. This exceptional antioxidant performance is attributed to a hydrogen-atom-transfer mechanism mediated by the densely functionalized carbon dot surface, complemented by a single-electron-transfer contribution from the aromatic sp^2 core. Collectively, these findings establish *L. hexandra* as a novel, abundant and cost-free precursor for the sustainable synthesis of high-performance antioxidant carbon dots, offering a dual benefit of agricultural weed valorization and the development of a green, biocompatible nanomaterial with promising

applications in food preservation, cosmeceuticals and biomedical antioxidant therapeutics. Future work should extend this study to include particle size and morphology analysis (e.g., TEM), quantum yield determination, excitation-dependent emission mapping, in vitro cytotoxicity and cellular antioxidant assays, and pilot-scale process optimization to fully realize the translational potential of this waste-to-wealth nanomaterial.

Funding Information: "This research did not receive any specific grant from funding agencies in the public, commercial, or not-for-profit sectors."

Declaration of Conflict: The authors declare no conflict of interest.

REFERENCES

1. Xu, X., Ray, R., Gu, Y., Ploehn, H. J., Gearheart, L., Raker, K., & Scrivens, W. A. (2004). Electrophoretic analysis and purification of fluorescent single-walled carbon nanotube fragments. Journal of the American Chemical Society, 126(40), 12736-12737.
2. Chopra, A., Kumari, Y., Singh, A. P., & Sharma, Y. (2024). A review on green synthesis, biological applications of carbon dots in the field of drug delivery, biosensors, and bioimaging. Luminescence, 39(8), e4870.
3. Shahraki, H. S., Ahmad, A., & Bushra, R. (2022). Green carbon dots with multifaceted applications–Waste to wealth strategy. FlatChem, 31, 100310.
4. Dubey, P. (2023). An overview on animal/human biomass-derived carbon dots for optical sensing and bioimaging applications. RSC advances, 13(50), 35088-35126.
5. Kanwal, A., Bibi, N., Hyder, S., Muhammad, A., Ren, H., Liu, J., & Lei, Z. (2022). Recent advances in green carbon dots (2015–2022): synthesis, metal ion sensing, and biological applications. Beilstein Journal of Nanotechnology, 13(1), 1068-1107.
6. Luo, J., Ma, Y., Chen, W., & Pang, J. (2026). Green synthesis of biomass carbon nanodots and their multifunctional applications. Bioresource Technology, 134292.
7. Hasan, M., Baheerathan, B., Sutradhar, S., Shahbandinejad, R., Rakshit, S., Kozinski, J., ... & Kang, K. (2025). Microwave-assisted synthesis of biomass-derived N-doped carbon dots for metal ion sensing. Carbon research, 4(1), 49.
8. Wan, F. H., & Yang, N. W. (2016). Invasion and management of agricultural alien insects in China. Annual Review of Entomology, 61(1), 77-98.
9. Ji, Z., Sheardy, A., Zeng, Z., Zhang, W., Chevva, H., Allado, K., ... & Wei, J. (2019). Tuning the functional groups on carbon nanodots and antioxidant studies. Molecules, 24(1), 152.
10. Kasif, M., Alarifi, A., Afzal, M., & Thirugnanasambandam, A. (2024). N, S-codoped carbon dots for antioxidants and their nanovehicle potential as molecular cargoes. RSC advances, 14(44), 32041-32052.
11. Coroaba, A., Ignat, M., Carp, O. E., Stan, C. S., Filipiuc, S. I., Uritu, C. M., ... & Ania, C. O. (2025). Antioxidant activity and in vitro fluorescence imaging application of N-, O-functionalized carbon dots. Scientific Reports, 15(1), 25834.
12. Navarro-Badilla, A., Calderon-Ayala, G., Delgado-Beleño, Y., Heras-Sánchez, M. C., Hurtado, R. B., Leal-Pérez, J. E., ... & Cortez-Valadez, M. (2023). Green synthesis for carbon quantum dots via Opuntia ficus-indica and Agave maximiliana: surface-enhanced Raman scattering sensing applications. ACS omega, 8(37), 33342.
13. Aouadi, A., Saoud, D. H., Bouafia, A., Mohammed, H. A., Gamal, H. G., Achouri, A., ... & Al-Lohedan, H. A. (2025). Unveiling the antioxidant power: synthesis and characterization of lemon and orange peel-derived carbon quantum dots with exceptional free radical scavenging activity. Biomass Conversion and Biorefinery, 15(6), 9691-9704.
14. Dager, A., Uchida, T., Maekawa, T., & Tachibana, M. (2019). Synthesis and characterization of mono-disperse carbon quantum dots from fennel seeds: photoluminescence analysis using machine learning. Scientific reports, 9(1), 14004.
15. Dager, A., Baliyan, A., Kurosu, S., Maekawa, T., & Tachibana, M. (2020). Ultrafast synthesis of carbon quantum dots from fenugreek seeds using microwave plasma enhanced decomposition: application of C-QDs to grow fluorescent protein crystals. Scientific reports, 10(1), 12333.

16. Zhao, K., Huang, Z., Saed, Y. A., Sun, X., & Zheng, Z. (2026). Biomass derived carbon dots from green synthesis to multimodal bioimaging applications. Discover Nano, 21(1), 282.
17. Mintz, K. J., Bartoli, M., Rovere, M., Zhou, Y., Hettiarachchi, S. D., Paudyal, S., ... & Leblanc, R. M. (2021). A deep investigation into the structure of carbon dots. Carbon, 173, 433-447.
18. Pan, Z., Zhou, Y., Ji, B., Liu, Q., & Fan, Z. (2026). Antioxidant performance and characterization comparison of carbon dots derived from agricultural waste pineapple peel. Foods, 15(2), 189.
19. Famutimi, O. G., Masha, S., Maluleke, R., Ncapayi, V., Lebepe, T. C., Mgedle, N., ... & Oluwafemi, O. S. (2025). Assessment of antioxidant potential of carbon-based nanomaterials from different sources. Antioxidants, 14(10), 1227.
20. Meng, L., Ding, P., Ou, M., & Zhang, Y. (2026). Houttuynia cordata-DES carbon quantum dots for Cr6+ detection and biological applications. Chemical and Biological Technologies in Agriculture, 13(1), 1.
21. Aji, M. P., Octaviani, A. C., Umar, S. R., Arrosyid, M. H., Maulina, D., Masturi, M., ... & Nuryadin, B. W. (2026). Carbon dots nanoparticles derived from showy Asian grapes (Medinilla speciosa) for free radical scavenger. Materials Science and Technology, 42(2), 191-201.
22. Peng, J., Hu, C., Zhou, X., Wu, D., Sun, X., Tang, A., ... & Tian, J. (2025). Synthesis and properties of carbon quantum dots: Antioxidant, antibacterial and pH response monitoring applications. Chemical Physics, 594, 112658.
23. Verma, S., Bhatt, M., & Das, B. (2025). Effect of carbon nanodots on the cellular redox reaction and immune system. Nanoscale advances, 7(7), 1784-1802.

HOW TO CITE: Shyamala Chandra Rokkala[1]*, Amal Joseph PJ[2], Waste-To-Wealth Valorization Of The Invasive Grass Leersia Hexandra Into Fluorescent Carbon Dots Via Microwave-Assisted Synthesis: Multi-Technique Characterization And DPPH Radical-Scavenging Potential, Int. J. Sci. R. Tech., 2026, 3 (9), 425-435. https://doi.org/10.5281/zenodo.22911103